Temporal characteristics of CH_4 vertical profiles observed in the West Siberian Lowland over Surgut from 1993 to 2015 and Novosibirsk from 1997 to 2015

M. Sasakawa[1], T. Machida[1], K. Ishijima[2], M. Arshinov[3], P. K. Patra[2], A. Ito[1], S. Aoki[4], and V. Petrov[5]

[1]Center for Global Environmental Research, National Institute for Environmental Studies, Tsukuba, Japan. 2, 3, ,

[2]Research Institute for Global Change, JAMSTEC, Yokohama, Japan.

[3]V.E. Zuev Institute of Atmospheric Optics, Russian Academy of Sciences, Siberian Branch, Tomsk, Russia.

[4]Center for Atmospheric and Oceanic Studies, Graduate School of Science, Tohoku University, Sendai, Japan.

[5]Central Aerological Observatory, ROSHYDROMET, Dolgoprudny, Russia.

Corresponding author: Motoki Sasakawa (sasakawa.motoki@nies.go.jp)

Key Points:

- The vertical gradients in methane concentrations observed over Surgut in West Siberia decreased because emissions from Europe decreased.
- Basic information of long-term aircraft observation over Surgut and Novosibirsk in the West Siberian Lowland is described.
- Vertical profile observations may validate the changing emissions at downwind of any region where a substantial change occurs.

Abstract

We have carried out monthly flask sampling using aircraft, in the altitude range of 0-7 km, over the boreal wetlands in Surgut (61ºN, 73ºE; since 1993) and a pine forest near Novosibirsk (55ºN, 83ºE; since 1997), both located in the West Siberian Lowland (WSL). The temporal variation of methane (CH_4) concentrations at all altitudes at both sites exhibited an increasing trend with stagnation during 2000-2006 as observed globally from ground-based networks. In addition to a winter maximum as seen at other remote sites in northern mid to high latitudes, another seasonal maximum was also observed in summer, particularly in the lower altitudes over the WSL, which could be attributed to emissions from the wetlands. Our measurements suggest that the vertical gradient at Surgut has been decreasing; the mean CH_4 difference between 5.5 km and 1.0 km changed from 64±5 ppb during 1995-1999 to 37±3 ppb during 2009-2013 (mean ± standard error). No clear decline in the CH_4 vertical gradient appeared at Novosibirsk. Simulations using an atmospheric chemistry-transport model captured the observed decrease in the vertical CH_4 gradient at Surgut when CH_4 emissions from Europe decreased but increased from the regions south of Siberia, e.g., East and South Asia. At Novosibirsk, the influence of the European emissions was relatively small. Our results also suggest that the regional emissions around the WSL did not change significantly over the period of our observations.

1. Introduction

Similarly to carbon dioxide (CO_2), concentrations of other trace gasses of anthropogenic origin have risen significantly since the industrial revolution. Atmospheric CH_4 showed an increasing trend with stagnation from 2000 to 2006, whose causes have frequently been debated in recent years [*Dlugokencky et al.,* 2003; *Rigby et al.,* 2008; *Kirschke et al.,* 2013; *Patra et al.,* 2016; *McNorton et al.,* 2016a, 2016b; *Saunois et al.,* 2016]. Methane concentration in the troposphere is principally determined by a balance of surface emissions, atmospheric transport, and destruction by hydroxyl (OH) radicals [*Patra et al.,* 2011]. Emission sources comprise anthropogenic activities such as agriculture and waste, fossil fuels, and biomass burning, and natural sources such as wetlands, fresh water ecosystems, wild animals, and geological and oceanic sources [*Saunois et al.,* 2016]. The stagnation and the subsequent regrowth of globally observed CH_4 concentration could be attributed to the temporal variation in the strength of the primary source (agriculture and waste, fossil fuels, and wetlands). The role of sink processes is less explored due to poor quantification of the interannual and inter-decadal variations in OH [*Naik et al.,* 2013; *McNorton et al.,* 2016a].

Interestingly, the carbon isotopic signature of CH_4 clearly changed after the regrowth, which implies that biogenic emissions considerably increased after the stagnation [*Schaefer et al.,* 2016; *Nisbet et al.,* 2016]. Using regional emissions inversion, *Patra et al.* [2016] estimated that the CH_4 emissions from the tropical and Southern Hemisphere regions increased by ~10 Tg yr^{-1} from 2004 to 2012. Based on the statistics of cattle stocks and the carbon isotopic signature, the authors concluded that the increase was due to enteric fermentation. This increased amount is incidentally similar to the emissions from the East Asian region (mainly China) due to the coal industry. *Schaefer et al.* [2016] rejected the hypothesis that wetland emissions had been the primary cause of CH_4 regrowth and suggested that regrowth had been driven by agricultural emissions. On the contrary, *Nisbet et al.* [2016] proposed that tropical wetlands, as well as tropical agricultural emissions, were likely the dominant contributors to recent growth. Using a land surface model which included an improved representation of topography, *McNorton et al.* [2016b] estimated wetland CH_4 emissions from 1993 to 2014 and showed that global wetland

emissions made only a small contribution to the pause in CH_4 growth from 1999 to 2006. Their study further suggested that the increased growth after 2006 was caused partly by increased wetland emissions mainly from Tropical Asia, Southern Africa, and Australia.

Using column data of ethane (C_2H_6) and CH_4 at two observatories in the northern and Southern Hemispheres during 1999-2014, *Hausmann et al.* [2016] estimated that the contribution of fossil fuel emissions to the renewed CH_4 increase was 39 % at a minimum. With C_2H_6 data from a large number of monitoring sites, *Helmig et al.* [2016] also found that the steady decline in the C_2H_6 mole fraction halted between 2005 and 2010 in most of the northern hemisphere and had since reversed, which suggested the significant increase in associated CH_4 emissions from fossil fuel. As shown above, however, the increase in fossil fuel emissions is inconsistent with the changed carbon isotopic signature.

Recently, a manuscript to focus on quasi-decadal and inter-annual variability in CH_4 emissions using the Global Carbon Project (GCP) dataset [Saunois et al., 2016] has been reviewed [Saunois et al., 2017]. In this manuscript, the ensemble of top-down studies provided by eight global inverse systems suggested a dominant contribution to the global emission increase from agriculture and waste (+10 [7-12] Tg CH_4 yr^{-1}), wetlands (+6 [-4-16] Tg CH_4 yr^{-1}), and fossil fuel-related emissions (+7 [-2-16] Tg CH_4 yr^{-1}) from 2000-2006 to 2008-2012. Saunois et al. [2017] also showed that the decrease of biomass burning emissions (-3 [-7-0] Tg CH_4 yr^{-1}) could be consistent with the carbon isotopic signature. The uncertainties of these mean emission changes are, however, very significant as shown by the range inferred by eight inversions. In summary, the cause of the stagnation and subsequent regrowth of atmospheric CH_4 and its attribution to different sources are still not fully resolved.

The role of Siberia in the global CH_4 budget is essential because it contains vast areas of natural wetland and numerous oil and gas fields that release significant amounts of natural gas as a result of leakage during fossil fuel production and transportation. Studies of CH_4 behaviour and attempts to identify sources of variation have been conducted over Siberia by means of observations from aircraft [*Sugawara et al.,* 1996; *Tohjima et al.,* 1996, 1997; *Nakazawa et al.,* 1997; *Levin et al.,* 2002; *Lloyd et al.,* 2002; *Yamada et al.,* 2005; *Umezawa et al.,* 2012], the Trans-Siberian Railway [*Bergamaschi et al.,* 1998; *Tarasova et al.,* 2006], tower sites [*Kozlova et al.,* 2008; *Winderlich et al.,* 2010; *Sasakawa et al.,* 2010, 2012; *Dlugokencky et al.,* 2016]. However, most of these observations were limited to short periods or a specific season.

To capture the seasonal cycles, vertical profiles, and long-term trends of greenhouse gases, the Center for Global Environmental Research (CGER) of the National Institute for Environmental Studies (NIES) of Japan, in cooperation with ROSHYDROMET and the Russian Academy of Sciences (RAS), began periodic flask sampling using aircraft over Surgut (61°N, 73°E) in 1993, over Yakutsk (62°N, 129°E) in 1996, and over Novosibirsk (55°N, 83°E) in 1997. A part of the observed data for CO_2 [*Saeki et al.,* 2013], CH_4 [*Saito et al.,* 2013], and N_2O [*Ishijima et al.,* 2010] was used for inversion analysis or validation of an atmospheric chemistry transport model. The observed CH_4 concentration also validated the column-averaged dry air mole fractions of CH_4 obtained by the Greenhouse gases Observing SATellite (GOSAT) [*Ono et al.,* 2015] and was used for bias correction of satellite retrieval [*Tan et al.,* 2016]. The present paper is the first paper to present a comprehensive description of the aircraft observations of CH_4 concentrations during 1993-2015 over Surgut and 1997-2015 over Novosibirsk in the WSL, where long-term continuous observations were conducted in the same manner. The objective of this paper is to (1) describe the observational method for further use of the datasets, (2) provide analyses of the CH_4 time series for seasonal cycle, interannual variations, and long-term trends,

and (3) offer an interpretation of the observations using simulations by means of an atmospheric chemistry transport model.

2. Method

2.1 Sample area description

Research flights for flask sampling in the Surgut region have been undertaken within 130 km of Surgut which is one of the most important centers of oil and gas production in West Siberia. It is located in Khanty-Mansi Autonomous Area - Yugra, in the central part of the WSL. The landscape zone is a middle taiga transiting to northern taiga. Vast areas of the region under study are covered by the peatland system "Surgutskoe Polesye" which consists of numerous peatland-lake complexes parted by river valleys [Terentieva et al., 2016]. The climate is continental subarctic. The mean annual air temperature is about minus 2.5°C. Average seasonal temperatures are: -20 °C (DJF), -3°C (MAM), +15°C (JJA), and -2°C (SON). Prevailing winds blow from the southwest.

Air sampling in the Novosibirsk region has been performed over the National Karakan Pine Forest located on the right bank of Novosibirsk Reservoir (Ob River). The area under study is situated in the southeast of the West Siberian Plain. The typical landscape is a forest-steppe. Numerous lakes, marshes, floodplains are also important elements of the region. The type of climate is humid continental. Prevailing winds are from the south and southwest. The mean annual air temperature over the study period (1997-2015) was +2.1 °C with inter-annual anomalies ranging from +1.4°C to -1.5°C which were caused predominantly by winter temperatures (Figure S1). The growing season lasts for about 160 days.

2.2 Air sample collection

Air sampling has been carried out approximately once per month using a chartered aircraft (Antonov An-24) at the altitudes of 7.0, 5.5, 4.0, 3.0, 2.0, 1.5, 1.0, and 0.5 km within 130-km distance from Surgut since July 23, 1993. Air was sampled upwind of Surgut to avoid direct contamination from the city. Two samples were collected at each altitude during the level flight, and the sampling interval was 2-3 minutes. It took 40-50 minutes to collect all samples from 7.0 to 0.5 km. Flights were performed around noon or in the afternoon of local time. The air sample was introduced into the cockpit through an inlet placed in front of the engine exhaust and pressurized into a Pyrex glass flask at about +0.2 MPa over cabin pressure by using an electric diaphragm pump (MOA-P101-JH or DOA-P501, GAST Manufacturing Inc.). The flask sizes have varied from 550 mL until 22 February 2005, to 500 mL and 750 mL until 26 April 2012, and are recently maintained at 750 mL. Before use, the flasks were washed using an ultrasonic cleaner filled with purified water and then dried for at least 6 hours at 100°C temperature. The stopcocks of the glass flasks and the diaphragm pump were operated manually.

Until 2005 February, the air samples from Surgut were sent to Tohoku University and analyzed for CH_4 concentration using a gas chromatograph equipped with flame ionization detector (GC-FID). The GC systems used were a GC-9A (Shimadzu Corp.) in earlier years and then an Agilent 6890 (Agilent Technologies, Inc.) since November 2002. Each gas sample was analyzed once or twice. Repetitive calibrations using multiple CH_4 standard gas mixtures indicated that repeatability of our measurements was 3 ppb for the GC-9A and 2 ppb for the Agilent 6890 system [*Umezawa et al.,* 2014]. The CH_4 concentration was determined against the TU scale [*Aoki et al.,* 1992], which is ~3.2 ppb higher than the WMO-CH4-X2004 scale in the

concentration range of 1755.5-1820.2 ppb (Round Robin Comparison Experiment; http://www.esrl.noaa.gov/gmd/ccgg/wmorr/).

After March 2005, the air samples were sent to NIES and analyzed for CH_4 concentration using GC-FID as well. The system used was HP5890 (Hewlett-Packard Comp.) until April 2014, followed by Agilent 7890A (Agilent Technologies, Inc.) for the samples collected after 24 April 2014. Each gas sample was analyzed three times. The precision was 1.7 ppb in both systems. The concentration was determined against NIES 94 CH_4 scale, which is ~3.7 ppb higher than the WMO-CH4-X2004 scale in the concentration range of 1755.5-1820.2 ppb (Round Robin Comparison Experiment). Both the TU and NIES scales showed good agreement in their precision.

Air sampling over the pine forest area about 150 km southwest of Novosibirsk, had been conducted approximately once per month since July 23, 1997, using a research plane (Antonov An-30) operated by the Institute of Atmospheric Optics [*Antokhin et al.,* 2012]. We have used a chartered aircraft (Tupolev Tu-134) since March 25, 2011. The air samples had been collected in 500-mL Pyrex glass flasks and sent to NIES for analysis of CH_4 concentration using GC-FID. We started to use 750-mL flasks on June 30, 1999, and used them together with 500-mL flasks until March 2004. Since March 17, 2004 we have used only 750-mL flasks. The system used was first HP5890 (Hewlett-Packard Comp.), followed by Agilent 7890A (Agilent Technologies, Inc.) from the samples obtained on March 18, 2014. Other sampling procedures and conditions were almost the same as those conducted over Surgut (Table 1).

2.3 Tagged tracer simulations

To specify which source regions affected CH_4 concentrations at different altitudes of our air sampling, tagged tracer experiments were performed using the Japan Agency for Marine-Earth Science and Technology's Atmospheric Chemistry Transport Model (JAMSTEC's ACTM) [*Patra et al.,* 2009, 2016] in the same manner as in *Umezawa et al.,* [2012]. We have used the CH_4ags case of the surface emissions based on a 53-region time-dependent inverse model using the ACTM as the forward model [*Patra et al.,* 2016]. The ACTM is run at a horizontal resolution of T42 spectral truncations (~2.8 x 2.8º), and 67 sigma-pressure vertical levels. The surface flux field was divided into 18 regions of the globe (Figure 1), and each CH_4 tracer was simulated separately with the region's flux field. The model was spun-up by repeating the simulation of the year 2000 about 20 times until no more changes in the regional tracer concentrations occurred. In this process, the simulated values at the end of 2000 were used as the initial values on 1 Jan 2000 for the next simulation, and the sum of the global mean surface concentrations of all the regional tracers was every time scaled to the observed global mean on 1 Jan 2000 by applying a single scaling factor to all tracers. We confirmed that the sum of the 18 tracers and the simulated concentration with the total global flux field agreed with each other within 0.1 %. The ACTM assumes that CH_4 is removed from the atmosphere by reaction with OH, Cl and $O(^1D)$ and transported globally. The concentrations of the reactants were prescribed by independent modeling results at monthly time intervals [*Spivakovsky et al.,* 2000; *Takigawa et al.,* 1999]. The OH and Cl concentrations varied seasonally, but the seasonality was repeated every year. Global CH_4 emissions for the observation period (2001-2013) varied from 503 to 526 Tg yr^{-1}. The model's meteorological field was nudged to Japanese 25-year Re-Analysis (JRA25) [*Onogi et al.,* 2007] and was, thus, inter-annually variable. *Patra et al.,* [2016] showed that the 53-region inverted emission and the ACTM simulations successfully simulated the independent CH_4 observations by Tohoku University over Japan within 5 ppb and the HIPPO measurements over

the central Pacific Ocean within 3 ppb, which are close to the measurement uncertainty. We also confirmed that the variations in CH_4 concentrations observed at surface baseline sites around the world were reproduced well by using this model (Figure S2, S3). We interpolated temporally, horizontally, and vertically the hourly model outputs to match the collection time of each flask over Surgut and Novosibirsk to compare the model results with the observational results.

2.4 Data analysis

For the samples measured repeatedly, we set a criterion that the standard deviation (SD) of repeated measurements of less than two times of the precision was valid (dependent on the GC systems); i.e. we did not use the samples whose SD was bigger than 6 ppb (~Oct. 2002), 4 ppb (Nov. 2002~Feb. 2005), and 3.4 ppb (Mar. 2005~). We thus analyzed 3686 samples for Surgut and 2943 samples for Novosibirsk. The data are available from the Global Environmental Database, hosted by CGER, NIES (http://db.cger.nies.go.jp/portal/geds/index).

Stratosphere-troposphere exchange (STE) is one of the important factors controlling the CH_4 concentrations in the upper troposphere [*Umezawa et al.,* 2014]. It is known that the N_2O concentration has a sharp gradient around the tropopause, allowing us to detect STE events by looking for low N_2O concentrations [*Ishijima et al.,* 2010; *Assonov et al.,* 2013]. As shown in *Umezawa et al.* [2014], we also sorted STE-influenced data based on low N_2O concentrations measured concurrently. Detection of STE-influenced samples was made as follows. The temporal variation in N_2O concentrations from each sample at the respective altitudes was detrended using curve fitting methods which consist of a function fit to the data, and digital filtering of the residuals from the fit, developed by NOAA-ESRL (http://www.esrl.noaa.gov/gmd/ccgg/mbl/crvfit/crvfit.html). The filtering method is used to transform the data into the frequency domain using a Fast Fourier Transform (FFT), apply a low pass filter function to the frequency data, then transform the filtered data to the real domain using an inverse FFT. We applied a Python code for computing the filtering method, which is available at ftp://ftp.cmdl.noaa.gov/user/thoning/ccgcrv/. Histograms of the detrended N_2O at lower altitudes could be approximated by the normal distribution with a width (sigma) of up to 1.1 ppb during the measurement at Tohoku University and 0.5 ppb during the measurement at NIES (Figure S4, S5, S6). Histograms at higher altitudes were skewed to the lower concentration side due to some STE-influenced samples. Some data in the lowest altitude of 0.5 km distributed in the higher concentration side were likely due to local sources from the surface. The N_2O concentration data lower than the long-term trend by more than 3.3 ppb (1.4 ppb), i.e. 3-sigma at lower altitudes, were defined as STE-influenced samples measured at Tohoku University (NIES). Our N_2O criterion was close to that in *Assonov et al.,* [2013] (1.0 ppb) and that in *Umezawa et al.* [2014] (2.7 ppb). We iterated the same method for the residual data and further defined STE-influenced samples (Figure S7, S8). After three iterations, no STE-influenced sample remained. To describe CH_4 characteristics under normal conditions of the troposphere, we did not use the corresponding CH_4 data of the STE-influenced samples (48 samples at Surgut; 35 samples at Novosibirsk) for the calculation of curve fitting, and thus, excluded the data from subsequent discussions. The average of CH_4 concentrations from residual samples (3638 samples at Surgut; 2908 samples at Novosibirsk) obtained at the same altitude on a certain date was regarded as representative data of the altitude on that date. The number of average data was 1933 for Surgut and 1498 for Novosibirsk.

Although air sampling was carried out approximately once per month, the timing was not exactly periodical, and occasionally there was no sample taken in a month. Thus, to estimate the

error in the calculated long-term trend, we used a bootstrap method in which 100 data sets with equal sizes to the original data sets (220-247 for Surgut and 185-189 for Novosibirsk at each altitude) were prepared by random resampling. Note that there were overlapped data in each bootstrap data set. We calculated the long-term trend for each of the 100 datasets at each altitude by the same method and determined the error as the SD of the 100 values.

3. Results and Discussion

3.1 Long-term variation and seasonality

The temporal variation in CH_4 concentrations at the observed altitudes over Surgut and Novosibirsk is shown in Figure 2 and Figure S9, respectively. Just as *Ishijima et al.* [2010] reported that stratospheric air contributed to the variation of tropospheric N_2O in the 0.5-7 km altitude range at Surgut, some of our samples, particularly at 7.0 km in altitude, were affected by stratospheric intrusion (Fig. S7, S8). Most of them showed notably lower CH_4 values. Tropospheric CH_4 concentrations were higher with larger variability at lower altitudes due to strong CH_4 emissions from the ground surface. During our observation periods, the long-term trend in globally-averaged CH_4 concentrations observed at a globally distributed network by NOAA (www.esrl.noaa.gov/gmd/ccgg/trends_ch4/) showed an increase in the period of 1994-1999 (2.17 ± 0.52 to 11.99 ± 0.68 ppb yr^{-1}), stagnation of growth rate in the period of 2000-2006 (-4.55 ± 0.43 to 4.60 ± 0.68 ppb yr^{-1}), and regrowth in the period of 2007-2015 (4.63 ± 0.46 to 12.60 ± 0.47 ppb yr^{-1}). We showed the long-term trends in CH_4 concentrations with the cutoff frequencies of 667, 1095, 1460 days in the low pass filter (Figure 2, Figure S9). Regardless of the cutoff frequencies in the low pass filter, the general long-term trends in the higher altitudes observed over Surgut and Novosibirsk were roughly consistent with those of globally-averaged CH_4. At Surgut, significant growth rates appeared in the period of 1997-1998 followed by a negative trend around 1999-2001 (Figure 3). A positive trend then appeared even in the period of 2000-2006, which continued after the year of 2007. At Novosibirsk, small or negative trends in the growth rates appeared in the period of 2000-2005 followed by regrowth since 2006. These variations in the long-term trends at both sites suggest a dominant influence of the global CH_4 budget on the observed long-term CH_4 trend because emission signals even from the Southern Hemisphere take only about one year to reach the northern hemisphere, as defined by the inter-hemispheric exchange time of ~1.4 yr [*Patra et al.,* 2011]. On the other hand, the growth rates observed in the lower altitudes at both sites sometimes showed a different tendency with great variability from those obtained at the network by NOAA. This is due to the larger variability in CH_4 concentrations induced by influence from ground emissions around Surgut and Novosibirsk compared to the weak CH_4 variability at the remote stations considered in the NOAA global mean calculation. Note that the variability in growth rate could be enhanced if a shorter cutoff frequency was applied; the cutoff frequency of 1460 days was applied in Figure 3.

A slight seasonality with a summer minimum was observed in the altitudes of 5.5 km and 4 km over Surgut as similar to those observed at global background sites [e.g. Nisbet et al., 2016] (Figure 4). On the other hand, a distinctive seasonality with two maxima, one in winter (January at 1 km and 0.5 km, and March at 3 km, 2 km, and 1.5 km) and one in summer (July or August), appeared below 3 km as observed at tower sites in the WSL [*Sasakawa et al.,* 2010]. Generally, CH_4 emissions from the wetlands in the WSL increase during summer at the same time as the height of planetary boundary layer (PBL) develops well. The PBL height in the WSL sometimes exceeded 3 km in altitude during summer [*Sasakawa et al.,* 2013]. Thonat et al. [2017] showed increased CH_4 concentration at the East Siberian site (Tiksi) during summer and found that CH_4

from Arctic wetlands contributed by 36 ppb on average to the CH_4 concentration estimated by a chemistry-transport model, which also revealed that CH_4 loss by oxidation with OH radicals could be 11 ppb at maximum in July. In Surgut, similarly, large CH_4 emissions from the wetlands in the WSL likely have exceeded the zonal-mean CH_4 loss by reaction with OH radicals, inducing the summer maximum below 3 km. From observations at altitudes of 2 km and 1 km over Surgut for the period of 2004-2009, *Umezawa et al.* [2012] could not catch any clear seasonal cycle in CH_4 concentrations, probably due to the limited amount of data of year-round observations (4 yr) and the high variability at lower altitudes. At the highest altitude (7 km), seasonality was not clear because the direct influence of emissions from the ground was relatively small and not-removed STE influence probably remained. In Novosibirsk, a summer maximum was observed below 2 km (Figure S10). However, the scatter in summer months was smaller than that in Surgut likely because Novosibirsk was relatively far from the wetlands situated in the northern part of the WSL. No clear seasonality appeared at higher altitudes.

Lloyd et al., [2002] observed the vertical profile of CH_4 below the altitude of 3 km over a tower in central Siberia during 1998-2000, and found a higher level and greater variability of the concentrations in the PBL than those in the free troposphere. Furthermore, a clear seasonality with a summer minimum appeared in the free troposphere above an estimated maximum PBL height of 2.8 km during summer. However, they did not observe any distinct seasonal pattern in the PBL, which might be the result of the characteristics of the place (taiga in central Siberia) or just the shorter observation period (<3 yr). The present manuscript is probably the first one to report the summer maximum in CH_4 concentrations at as high as 3 km in altitude over the WSL.

3.2 Regional contribution to the observed CH_4

The simulation results combining all emissions from the 18 regions are generally in agreement with the observed CH_4 concentrations within one SD on a monthly basis at each altitude over Surgut (Figure S11) and Novosibirsk (Figure S12), although the simulation results showed slightly lower values during summer (June-August). At both sites, the contributions from all the regions in which significant CH_4 sources are distributed (Europe, Africa, WSL, India, East Asia, Southeast Asia, Boreal North America, Temperate North America, South America in Figure 1) were dominant for the observation periods (Figure 5, S13). However, the primary factor for seasonal and short-term variations in CH_4 concentrations at 1 km over Surgut and Novosibirsk was CH_4 originating from Europe (Region 2) and the WSL (Region 5) (Figure S14, S15). For Surgut, the SDs of the detrended seasonal and short-term variation of each contribution at 1 km, revealed by the curve fitting methods (Section 2.4), demonstrated much higher values for the contributions from Europe (19 ppb) and the WSL (25 ppb) than from other regions (<5 ppb) for the simulation period. Similarly, the SDs for Novosibirsk showed higher values for the contributions from Europe (11 ppb) and the WSL (14 ppb) than from other regions (<4 ppb). Although the SDs at 5.5 km decreased, the SDs of the contributions from Europe (7 ppb for Surgut and 6 ppb for Novosibirsk) and from the WSL (5 ppb for Surgut and 4 ppb for Novosibirsk) were still the largest in all regions.

As to the long-term trend, an apparent increasing trend in the contributions from India (Region 7), East Asia (Region 9), and Southeast Asia (Region 12) was pronounced (Figure 6, S16), causing an increasing trend for the combined CH_4 concentration for Surgut and Novosibirsk. On the other hand, a decreasing trend appeared only in the contribution from Europe for both sites. It rarely happens that a transport pattern only from Europe changes dramatically in the decadal span. The annual cumulative value of used emissions from Europe

was 62.81 Tg in 2001 which decreased by 0.50±0.15 Tg yr^{-1} until 2013, suggesting that the decline in the emissions from Europe primarily produced the decrease in contribution from Europe instead of a change in transport pattern. The total CH_4 emissions from 38 European countries listed in the Emissions Database for Global Atmospheric Research showed a decreasing trend of -0.29±0.02 Tg yr^{-1} for the period of 2001-2012 [*EDGAR42FT,* 2014]. Recently, inversion results by Tsuruta et al. [2017] reported a reduction in anthropogenic CH_4 emissions from Europe by 0-3 Tg CH_4 yr^{-1} between 2000-2006 and 2008-2012. Thus, anthropogenic emissions from Europe seemed to be reduced for the period of 2001-2013 as well. The annual cumulative value of used emissions from the WSL showed a positive anomaly in 2007, but there was no apparent long-term trend in the period of 2001-2013.

3.3 Vertical gradient

The vertical gradient in CH_4 concentrations over Surgut decreased in 20 years (Figure 7b). For example, the mean vertical gradients, defined here by the difference in monthly mean values produced from the fitting method (Section 2.4), between 1 km and 5.5 km were 64 ± 5 ppb, 46 ± 3 ppb, and 37 ± 3 ppb in the period of 1995-1999, 2002-2006, and 2009-2013, respectively. The results of the tagged tracer simulation showed that the difference between 1 km and 5.5 km was seen in Surgut only for emissions from Europe (Region 2), the WSL (Region 5), and the Boreal North America (Region 15) which include significant CH_4 sources and lie in the same latitudinal zone as Surgut (Figure S14). Other regions did not produce any vertical gradient, indicating that CH_4 emitted from other latitudinal zones was relatively well mixed toward a vertical direction during long-range transport. Although there was no discernible long-term trend in the vertical gradient of CH_4 in Surgut from the WSL and the Boreal North America, the gradient from Europe exhibited a decreasing trend in recent years due to the declined emissions from Europe as mentioned above (Figure 7a). The sum of the mean vertical gradients between 1 km and 5.5 km in the contribution from Europe (22 ± 2 and 16 ± 2 ppb in 2002-2006 and 2009-2013, respectively) and the WSL (25 ± 3 and 22 ± 2 ppb in 2002-2006 and 2009-2013, respectively) can explain the observed gradients for the respective periods of 2002-2006 (46 ± 3 ppb) and 2009-2013 (37 ± 3 ppb) (Figure 7b).

There was no apparent tendency in the difference between the monthly means produced from the fitting method at 1 km and those at 5.5 km over Novosibirsk in 18 years (Figure 8b). The differences between the mean concentrations of the monthly means were 35 ± 2 ppb and 39 ± 3 ppb for the period of 2002-2006 and 2009-2013, respectively. As mentioned in Section 3.2, a major characteristic of the contribution from 18 regions at Novosibirsk was similar to that at Surgut (Figure S15, S16); the seasonal and short-term variations from Europe and the WSL were larger than those from other regions, and the contribution from Europe decreased in all altitudes. The mean vertical gradient between 1 km and 5.5 km in the contribution from Europe was, however, smaller (15 ± 1 ppb) than that at Surgut (22 ± 2 ppb) in 2002-2006. Consequently, the vertical gradient in Novosibirsk might exhibit less sensitivity to the reduction in CH_4 emissions from Europe. Bruhwiler et al. [2017] reported that a trend in emissions would impact the vertical gradient at a site depending on its proximity to the emissions. No discernible weakening vertical gradient in the observed CH_4 over Novosibirsk was found because Novosibirsk is situated relatively far from Europe.

4. Conclusions

We have measured the vertical profiles of CH_4 over boreal wetlands and taiga in West Siberia (Surgut and Novosibirsk) for several decades. We found a positive trend of the concentrations with a period of stagnation during 2000-2006 as observed globally. However, the increasing rate of the concentrations was somewhat different depending on the altitude, inducing a negative trend in the vertical gradient of the concentration over Surgut. The mean vertical gradient in the early period (1995-1999) was clearly steeper than that in the subsequent periods (Figure 9). The negative trend remained, and hence the mean CH_4 concentrations at the lower altitudes, particularly below 1.5 km altitude, got closer to the mean concentrations at higher altitudes from the period of 2002-2006 to 2009-2013. The simulation results combining our tagged tracer simulations from 18 partitions of the global emission map reproduced the decline in the vertical gradient. However, most of the contributions from the divided regions showed flat vertical profiles except for Europe, the WSL, and the Boreal North America. A significant difference appeared in the variations in the concentrations between higher and lower altitudes from the WSL and Europe, which produced the vertical gradient (Figure 9). The mean contribution below 1 km altitude influenced by the contribution from the WSL decreased from the period of 2002-2006 to 2009-2013, but the difference was in the range of errors because the contributions from the WSL demonstrated a significant variability in the lower altitudes. On the other hand, the mean vertical gradient below 2.0 km altitude from Europe became noticeable gentle from the period of 2002-2006 to 2009-2013. The contribution from the emissions from Europe has decreased since the start of the simulation (2001). It is reported that CH_4 emissions from Europe have decreased since the late 1980s [*Worthy et al.,* 2009, *EDGAR42FT,* 2014]. We thus concluded that the observed decreasing trend in the vertical gradient over Surgut was attributed mainly to the decreasing CH_4 emissions from Europe.

Over Novosibirsk, there was no apparent decreasing trend in the gradient (Figure S17). On the contrary, the vertical gradient became slightly significant below 3 km altitude from the period of 2002-2006 to 2009-2013. There was no obvious difference in the contribution from the WSL between the periods although the contribution increased only at 0.5 km altitude. Furthermore, the reduction in CH_4 emissions from Europe did not appear in the contribution over Novosibirsk. The vertical gradients produced by the contribution from Europe over Novosibirsk were relatively weak compared to those at Surgut in the corresponding period, which suggests less sensitivity to the emission change from Europe at Novosibirsk. Similarly to Surgut, the contributions from other regions exhibited flat vertical profiles in both periods. No clear explanation could thus be obtained for the variation in the vertical gradient observed over Novosibirsk.

Although there has been no clear description up to date of the emission trend limited to the WSL, a reduction of 2 Tg in the period of 1988-2005 in Siberia [*Worthy et al.,* 2009] and an increasing trend of 0.30 to 0.72 Tg yr^{-2} in the period of 2005-2013 in Russia [*Thompson et al.,* 2017] were reported. It is beyond the scope of this paper to determine the exact amount or tendency in emissions from the WSL. It should be mentioned, however, that the simulation results combined with all emissions from 18 regions, including the emissions from the WSL with no clear trend, reproduced the observed concentrations over Surgut and Novosibirsk in the period of 2001-2013.

Unfortunately, we could not produce any simulations before the year of 2000 when a drastic reduction in the vertical gradient was observed over Surgut because of lack of reliable emission map for inter-annual variations. In the early years, sporadic leakage from old facilities for gas and oil pipelines around Surgut might have been significant and likely have influenced

435 the CH_4 concentrations, particularly in the lower altitudes. The facilities of pipelines have been
436 gradually updated in recent years, and thus the leakage might be relatively small and steady
437 [*Reshetnikov et al.,* 2000]. Monitoring the vertical profile of CH_4 over Siberia for a decadal span
438 can help us detect the long-term variations in the emissions from northern Eurasia. Our findings
439 also suggest the possibility that other vertical profile observations may capture the change in
440 vertical gradient and validate the changing emissions at downwind of any region where a
441 substantial change in emissions is thought to be taking place, e.g. China, India, and South East
442 Asia.
443

444 **Acknowledgments and Data**

445

446 We thank Sergey Mitin (Institute of Microbiology, Russian Academy of Sciences) for
447 administrative support. The authors thank the staff of the Zuev Institute of Atmospheric Optics,
448 Russia and the Winogradsky Institute of Microbiology, Russia for supporting the air sampling
449 over Siberia. This research was supported by a fund for global environmental monitoring by
450 CGER, NIES. The used data are available from the Global Environmental Database, hosted by
451 CGER, NIES (http://db.cger.nies.go.jp/portal/geds/index).

452 **References**

453 Antokhin, P. N., M. Y. Arshinov, B. D. Belan, D. K. Davydov, E. V. Zhidovkin, G. A. Ivlev, A.
454 V. Kozlov, V. S. Kozlov, M. V. Panchenko, I. E. Penner, D. A. Pestunov, D. V. Simonenkov,
455 G. N. Tolmachev, A. V. Fofonov, V. S. Shamanaev, and V. P. Shmargunov (2012), Optik-É
456 AN-30 aircraft laboratory for studies of the atmospheric composition, *J. Atmos. Oceanic*
457 *Technol.,* 29, doi:10.1175/2011JTECHA1427.1.
458 Aoki, S., T. Nakazawa, S. Murayama, and S. Kawaguchi (1992), Measurements of atmospheric
459 methane at the Japanese Antarctic Station, Syowa, *Tellus B,* 44, doi:10.1034/j.1600-
460 0889.1992.t01-3-00005.x.
461 Assonov, S. S., C. A. M. Brenninkmeijer, T. Schuck, and T. Umezawa (2013), N_2O as a tracer of
462 mixing stratospheric and tropospheric air based on CARIBIC data with applications for CO_2,
463 *Atmos. Environ.,* 79, doi:10.1016/j.atmosenv.2013.07.035.
464 Bergamaschi, P., C. A. M. Brenninkmeijer, M. Hahn, T. Röckmann, D. H. Scharffe, P. J.
465 Crutzen, N. F. Elansky, I. B. Belikov, N. B. A. Trivett, and D. E. J. Worthy (1998), Isotope
466 analysis based source identification for atmospheric CH_4 and CO sampled across Russia using
467 the Trans-Siberian railroad, *J. Geophys. Res.,* 103, 8227-8235.
468 Bruhwiler, L. M., S. Basu, P. Bergamaschi, P. Bousquet, E. Dlugokencky, S. Houweling, M.
469 Ishizawa, H. Kim, R. Locatelli, S. Maksyutov, S. Montzka, S. Pandey, P. K. Patra, G. Petron,
470 M. Saunois, C. Sweeney, S. Schwietzke, P. Tans, and E. C. Weatherhead (2017), U.S. CH_4
471 emissions from oil and gas production: Have recent large increases been detected?, *J.*
472 *Geophys. Res.,* 122, doi:10.1002/2016JD026157.
473 Dlugokencky, E. J., S. Houweling, L. Bruhwiler, K. A. Masarie, P. M. Lang, J. B. Miller, and P.
474 P. Tans (2003), Atmospheric methane levels off: Temporary pause or a new steady-state?,
475 *Geophys. Res. Lett.,* 30, doi:10.1029/2003GL018126.
476 Dlugokencky, E.J., P.M. Lang, A.M. Crotwell, J.W. Mund, M.J. Crotwell, and K.W. Thoning
477 (2016), Atmospheric Methane Dry Air Mole Fractions from the NOAA ESRL Carbon Cycle

Cooperative Global Air Sampling Network, 1983-2015, Version: 2016-07-07, Path: ftp://aftp.cmdl.noaa.gov/data/trace_gases/ch4/flask/surface/.

EDGAR42FT (2014), European Commission, Joint Research Centre (JRC)/Netherlands Environmental Assessment Agency (PBL). Emission Database for Global Atmospheric Research (EDGAR), release EDGARv4.2 FT2012, http://edgar.jrc.ec.europa.eu.

Hausmann, P., R. Sussmann, and D. Smale (2016), Contribution of oil and natural gas production to renewed increase in atmospheric methane (2007-2014): top-down estimate from ethane and methane column observations, *Atmos. Chem. Phys.,* 16, doi:10.5194/acp-16-3227-2016.

Helmig, D., S. Rossabi, J. Hueber, P. Tans, S. A. Montzka, K. Masarie, K. Thoning, C. Plass-Duelmer, A. Claude, L. J. Carpenter, A. C. Lewis, S. Punjabi, S. Reimann, M. K. Vollmer, R. Steinbrecher, J. W. Hannigan, L. K. Emmons, E. Mahieu, B. Franco, D. Smale, and A. Pozzer (2016), Reversal of global atmospheric ethane and propane trends largely due to US oil and natural gas production, *Nat. Geosci.,* 9, doi:10.1038/ngeo2721.

Ishijima, K., P. K. Patra, M. Takigawa, T. Machida, H. Matsueda, Y. Sawa, L. P. Steele, P. B. Krummel, R. L. Langenfelds, S. Aoki, and T. Nakazawa (2010), Stratospheric influence on the seasonal cycle of nitrous oxide in the troposphere as deduced from aircraft observations and model simulations, *J. Geophys. Res.,* 115, doi:10.1029/2009JD013322.

Kirschke, S., P. Bousquet, P. Ciais, M. Saunois, J. G. Canadell, E. J. Dlugokencky, P. Bergamaschi, D. Bergmann, D. R. Blake, L. Bruhwiler, P. Cameron-Smith, S. Castaldi, F. Chevallier, L. Feng, A. Fraser, M. Heimann, E. L. Hodson, S. Houweling, B. Josse, P. J. Fraser, P. B. Krummel, J. -F. Lamarque, R. L. Langenfelds, C. Le Quéré, V. Naik, S. O'Doherty, P. I. Palmer, I. Pison, D. Plummer, B. Poulter, R. G. Prinn, M. Rigby, B. Ringeval, M. Santini, M. Schmidt, D. T. Shindell, I. J. Simpson, R. Spahni, L. P. Steele, S. A. Strode, K. Sudo, S. Szopa, G. R. van der Werf, A. Voulgarakis, M. van Weele, R. F. Weiss, J. E. Williams, and G. Zeng (2013), Three decades of global methane sources and sinks, *Nat. Geosci.,* 6, doi:10.1038/ngeo1955.

Kozlova, E. A., A. C. Manning, Y. Kisilyakhov, T. Seifert, and M. Heimann (2008), Seasonal, synoptic, and diurnal-scale variability of biogeochemical trace gases and O_2 from a 300-m tall tower in central Siberia, *Global Biogeochem. Cycles,* 22, doi:10.1029/2008GB003209.

Levin, I., P. Ciais, R. Langenfelds, M. Schmidt, M. Ramonet, K. Sidorov, N. Tchebakova, M. Gloor, M. Heimann, E. D. Schulze, N. N. Vygodskaya, O. Shibistova, and J. Lloyd (2002), Three years of trace gas observations over the EuroSiberian domain derived from aircraft sampling — a concerted action, *Tellus B,* 54, 696-712.

Lloyd, J., R. L. Langenfelds, R. J. Francey, M. Gloor, N. M. Tchebakova, D. Zolotoukhine, W. A. Brand, R. A. Werner, A. Jordan, C. A. Allison, V. Zrazhewske, O. Shibistova, and E. D. Schulze (2002), A trace-gas climatology above Zotino, central Siberia, *Tellus B,* 54, 749-767.

McNorton, J., M. P. Chipperfield, M. Gloor, C. Wilson, W. Feng, G. D. Hayman, M. Rigby, P. B. Krummel, S. O'Doherty, R. G. Prinn, R. F. Weiss, D. Young, E. Dlugokencky, and S. A. Montzka (2016a), Role of OH variability in the stalling of the global atmospheric CH_4 growth rate from 1999 to 2006, *Atmos. Chem. Phys.,* 16, doi:10.5194/acp-16-7943-2016.

McNorton, J., E. Gloor, C. Wilson, G. D. Hayman, N. Gedney, E. Comyn-Platt, T. Marthews, R. J. Parker, H. Boesch, and M. P. Chipperfield (2016b), Role of regional wetland emissions in atmospheric methane variability, *Geophys. Res. Lett.,* doi:10.1002/2016GL070649.

Naik, V., A. Voulgarakis, A. M. Fiore, L. W. Horowitz, J. - Lamarque, M. Lin, M. J. Prather, P. J. Young, D. Bergmann, P. J. Cameron-Smith, I. Cionni, W. J. Collins, S. B. Dalsøren, R.

524 Doherty, V. Eyring, G. Faluvegi, G. A. Folberth, B. Josse, Y. H. Lee, I. A. MacKenzie, T.
525 Nagashima, T. P. C. van Noije, D. A. Plummer, M. Righi, S. T. Rumbold, R. Skeie, D. T.
526 Shindell, D. S. Stevenson, S. Strode, K. Sudo, S. Szopa, and G. Zeng (2013), Preindustrial to
527 present-day changes in tropospheric hydroxyl radical and methane lifetime from the
528 Atmospheric Chemistry and Climate Model Intercomparison Project (ACCMIP), *Atmos.*
529 *Chem. Phys.,* 13, doi:10.5194/acp-13-5277-2013.
530 Nakazawa, T., S. Sugawara, G. Inoue, T. Machida, S. Makshyutov, and H. Mukai (1997),
531 Aircraft measurements of the concentrations of CO_2, CH_4, N_2O, and CO and the carbon and
532 oxygen isotopic ratios of CO_2 in the troposphere over Russia, *J. Geophys. Res.,* 102, 3843-
533 3859.
534 Nisbet, E. G., E. J. Dlugokencky, M. R. Manning, D. Lowry, R. E. Fisher, J. L. France, S. E.
535 Michel, J. B. Miller, J. W. C. White, B. Vaughn, P. Bousquet, J. A. Pyle, N. J. Warwick, M.
536 Cain, R. Brownlow, G. Zazzeri, M. Lanoisellé, A. C. Manning, E. Gloor, D. E. J. Worthy, E.
537 Brunke, C. Labuschagne, E. W. Wolff, and A. L. Ganesan (2016), Rising atmospheric
538 methane: 2007–2014 growth and isotopic shift, *Global Biogeochem. Cycles,* 30,
539 doi:10.1002/2016GB005406.
540 Ono, A., S. Hayashida, T. Sugita, T. Machida, M. Sasakawa, and M. Arshinov (2015),
541 Comparison of GOSAT SWIR and aircraft measurements of XCH_4 over West Siberia, *SOLA,*
542 11, doi:10.2151/sola.2015-036.
543 Onogi, K., J. Tslttsui, H. Koide, M. Sakamoto, S. Kobayashi, H. Hatsushika, T. Matsumoto, N.
544 Yamazaki, H. Kaalhori, K. Takahashi, S. Kadokura, K. Wada, K. Kato, R. Oyama, T. Ose, N.
545 Mannoji, and R. Taira (2007), The JRA-25 reanalysis, *J. Meteor. Soc. Japan,* 85,
546 doi:10.2151/jmsj.85.369.
547 Patra, P. K., M. Takigawa, K. Ishijima, B. -C. Choi, D. Cunnold, E. J. Dlugokencky, P. Fraser,
548 A. J. Gomez-Pelaez, T. -Y. Goo, J. -S. Kim, P. Krummel, and R. Langenfelds (2009), Growth
549 rate, seasonal, synoptic, diurnal variations and budget of methane in the lower atmosphere, *J.*
550 *Meteor. Soc. Japan,* 87, doi:10.2151/jmsj.87.635.
551 Patra, P. K., S. Houweling, M. Krol, P. Bousquet, D. Belikov, D. Bergmann, H. Bian, P.
552 Cameron-Smith, M. P. Chipperfield, K. Corbin, A. Fortems-Cheiney, A. Fraser, E. Gloor, P.
553 Hess, A. Ito, S. R. Kawa, R. M. Law, Z. Loh, S. Maksyutov, L. Meng, P. I. Palmer, R. G.
554 Prinn, M. Rigby, R. Saito, and C. Wilson (2011), TransCom model simulations of CH_4 and
555 related species: linking transport, surface flux and chemical loss with CH_4 variability in the
556 troposphere and lower stratosphere, *Atmos. Chem. Phys.,* 11, doi:10.5194/acp-11-12813-2011.
557 Patra, P. K., T. Saeki, E. J. Dlugokencky, K. Ishijima, T. Umezawa, A. Ito, S. Aoki, S.
558 Morimoto, E. A. Kort, and A. Crotwell (2016), Regional methane emission estimation based
559 on observed atmospheric concentrations (2002-2012), *J. Meteor. Soc. Japan,* 94,
560 doi:10.2151/jmsj.2016-006.
561 Reshetnikov, A. I., N. N. Paramonova, and A. A. Shashkov (2000), An evaluation of historical
562 methane emissions from the Soviet gas industry, *J. Geophys. Res.,* 105,
563 doi:10.1029/1999JD900761.
564 Rigby, M., R. G. Prinn, P. J. Fraser, P. G. Simmonds, R. L. Langenfelds, J. Huang, D. M.
565 Cunnold, L. P. Steele, P. B. Krummel, R. F. Weiss, S. O'Doherty, P. K. Salameh, H. J. Wang,
566 C. M. Harth, J. Muehle, and L. W. Porter (2008), Renewed growth of atmospheric methane,
567 *Geophys. Res. Lett.,* 35, doi:ARTN L22805.
568 Saeki, T., S. Maksyutov, M. Sasakawa, T. Machida, M. Arshinov, P. Tans, T. J. Conway, M.
569 Saito, V. Valsala, T. Oda, R. J. Andres, and D. Belikov (2013), Carbon flux estimation for

Siberia by inverse modeling constrained by aircraft and tower CO_2 measurements, *J. Geophys. Res.,* 118, doi:10.1002/jgrd.50127.

Saito, R., P. K. Patra, C. Sweeney, T. Machida, M. Krol, S. Houweling, P. Bousquet, A. Agusti-Panareda, D. Belikov, D. Bergmann, H. Bian, P. Cameron-Smith, M. P. Chipperfield, A. Fortems-Cheiney, A. Fraser, L. V. Gatti, E. Gloor, P. Hess, S. R. Kawa, R. M. Law, R. Locatelli, Z. Loh, S. Maksyutov, L. Meng, J. B. Miller, P. I. Palmer, R. G. Prinn, M. Rigby, and C. Wilson (2013), TransCom model simulations of methane: Comparison of vertical profiles with aircraft measurements, *J. Geophys. Res.,* 118, doi:10.1002/jgrd.50380.

Sasakawa, M., K. Shimoyama, T. Machida, N. Tsuda, H. Suto, M. Arshinov, D. Davydov, A. Fofonov, O. Krasnov, T. Saeki, Y. Koyama, and S. Maksyutov (2010), Continuous measurements of methane from a tower network over Siberia, *Tellus B,* 62, doi:10.1111/j.1600-0889.2010.00494.x.

Sasakawa, M., A. Ito, T. Machida, N. Tsuda, Y. Niwa, D. Davydov, A. Fofonov, and M. Arshinov (2012), Annual variation of CH_4 emissions from the middle taiga in West Siberian Lowland (2005-2009): a case of high CH_4 flux and precipitation rate in the summer of 2007, *Tellus B,* 64, doi:10.3402/tellusb.v64i0.17514.

Sasakawa, M., T. Machida, N. Tsuda, M. Arshinov, D. Davydov, A. Fofonov, and O. Krasnov (2013), Aircraft and tower measurements of CO_2 concentration in the planetary boundary layer and the lower free troposphere over southern taiga in West Siberia: Long-term records from 2002 to 2011, *J. Geophys. Res.,* doi:10.1002/jgrd.50755.

Saunois, M., P. Bousquet, B. Poulter, A. Peregon, P. Ciais, J. G. Canadell, E. J. Dlugokencky, G. Etiope, D. Bastviken, S. Houweling, G. Janssens-Maenhout, F. N. Tubiello, S. Castaldi, R. B. Jackson, M. Alexe, V. K. Arora, D. J. Beerling, P. Bergamaschi, D. R. Blake, G. Brailsford, V. Brovkin, L. Bruhwiler, C. Crevoisier, P. Crill, K. Covey, C. Curry, C. Frankenberg, N. Gedney, L. Hoeglund-Isaksson, M. Ishizawa, A. Ito, F. Joos, H. -S. Kim, T. Kleinen, P. Krummel, J. -F. Lamarque, R. Langenfelds, R. Locatelli, T. Machida, S. Maksyutov, K. C. McDonald, J. Marshall, J. R. Melton, I. Morino, V. Naik, S. O'Doherty, F. -J. W. Parmentier, P. K. Patra, C. Peng, S. Peng, G. P. Peters, I. Pison, C. Prigent, R. Prinn, M. Ramonet, W. J. Riley, M. Saito, M. Santini, R. Schroeder, I. J. Simpson, R. Spahni, P. Steele, A. Takizawa, B. F. Thornton, H. Tian, Y. Tohjima, N. Viovy, A. Voulgarakis, M. van Weele, G. R. van der Werf, R. Weiss, C. Wiedinmyer, D. J. Wilton, A. Wiltshire, D. Worthy, D. Wunch, X. Xu, Y. Yoshida, B. Zhang, Z. Zhang, and Q. Zhu (2016), The global methane budget 2000-2012, *Earth Syst. Sci. Data,* 8, doi:10.5194/essd-8-697-2016.

Saunois, M., Bousquet, P., Poulter, B., Peregon, A., Ciais, P., Canadell, J. G., Dlugokencky, E. J., Etiope, G., Bastviken, D., Houweling, S., Janssens-Maenhout, G., Tubiello, F. N., Castaldi, S., Jackson, R. B., Alexe, M., Arora, V. K., Beerling, D. J., Bergamaschi, P., Blake, D. R., Brailsford, G., Bruhwiler, L., Crevoisier, C., Crill, P., Covey, K., Frankenberg, C., Gedney, N., Höglund-Isaksson, L., Ishizawa, M., Ito, A., Joos, F., Kim, H.-S., Kleinen, T., Krummel, P., Lamarque, J.-F., Langenfelds, R., Locatelli, R., Machida, T., Maksyutov, S., Melton, J. R., Morino, I., Naik, V., O'Doherty, S., Parmentier, F.-J. W., Patra, P. K., Peng, C., Peng, S., Peters, G. P., Pison, I., Prinn, R., Ramonet, M., Riley, W. J., Saito, M., Santini, M., Schroeder, R., Simpson, I. J., Spahni, R., Takizawa, A., Thornton, B. F., Tian, H., Tohjima, Y., Viovy, N., Voulgarakis, A., Weiss, R., Wilton, D. J., Wiltshire, A., Worthy, D., Wunch, D., Xu, X., Yoshida, Y., Zhang, B., Zhang, Z., and Zhu, Q.: Variability and quasi-decadal

changes in the methane budget over the period 2000–2012, Atmos. Chem. Phys. Discuss., https://doi.org/10.5194/acp-2017-296, in review, 2017.

Schaefer, H., S. E. M. Fletcher, C. Veidt, K. R. Lassey, G. W. Brailsford, T. M. Bromley, E. J. Dlugokencky, S. E. Michel, J. B. Miller, I. Levin, D. C. Lowe, R. J. Martin, B. H. Vaughn, and J. W. C. White (2016), A 21st-century shift from fossil-fuel to biogenic methane emissions indicated by $^{13}CH_4$, *Science,* 352, doi:10.1126/science.aad2705.

Spivakovsky, C. M., J. A. Logan, S. A. Montzka, Y. J. Balkanski, M. Foreman-Fowler, D. B. A. Jones, L. W. Horowitz, A. C. Fusco, C. A. M. Brenninkmeijer, M. J. Prather, S. C. Wofsy, and M. B. McElroy (2000), Three-dimensional climatological distribution of tropospheric OH: Update and evaluation, *J. Geophys. Res.,* 105, doi:10.1029/1999JD901006.

Sugawara, S., T. Nakazawa, G. Inoue, T. Machida, H. Mukai, N. K. Vinnichenko, and V. U. Khattatov (1996), Aircraft measurements of the stable carbon isotopic ratio of atmospheric methane over Siberia, *Global Biogeochem. Cycles,* 10, 223-231.

Takigawa, M., M. Takahashi, and H. Akiyoshi (1999), Simulation of ozone and other chemical species using a Center for Climate System Research/National Institute for Environmental Studies atmospheric GCM with coupled stratospheric chemistry, *J. Geophys. Res.,* 104, doi:10.1029/1998JD100105.

Tan, Z., Q. Zhuang, D. K. Henze, C. Frankenberg, E. Dlugokencky, C. Sweeney, A. J. Turner, M. Sasakawa, and T. Machida (2016), Inverse modeling of pan-Arctic methane emissions at high spatial resolution: what can we learn from assimilating satellite retrievals and using different process-based wetland and lake biogeochemical models?, *Atmos. Chem. Phys.,* 16, doi:10.5194/acp-16-12649-2016.

Tarasova, O. A., C. A. M. Brenninkmeijer, S. S. Assono, N. F. Elansky, T. Röckmann, and M. Braß (2006), Atmospheric CH_4 along the Trans-Siberian railroad (TROICA) and river Ob: Source identification using stable isotope analysis, *Atmos. Environ.,* 40, doi:10.1016/j.atmosenv.2006.04.065.

Terentieva, I. E., M. V. Glagolev, E. D. Lapshina, A. F. Sabrekov, and S. Maksyutov (2016), Mapping of West Siberian taiga wetland complexes using Landsat imagery: implications for methane emissions, *Biogeoscience*s, 13, 4615-4626, doi:10.5194/bg-13-4615-2016, 2016.

Thompson, R. L., M. Sasakawa, T. Machida, T. Aalto, D. Worthy, J. V. Lavric, C. Lund Myhre, and A. Stohl (2017), Methane fluxes in the high northern latitudes for 2005–2013 estimated using a Bayesian atmospheric inversion, *Atmos. Chem. Phys.,* 17, 3553-3572, doi:10.5194/acp-17-3553-2017.

Thonat, T., M. Saunois, P. Bousquet, I. Pison, Z. Tan, Q. Zhuang, P. M. Crill, B. F. Thornton, D. Bastviken, E. J. Dlugokencky, N. Zimov, T. Laurila, J. Hatakka, O. Hermansen, and D. E. J. Worthy (2017), Detectability of Arctic methane sources at six sites performing continuous atmospheric measurements, *Atmos. Chem. Phys.,* 17, doi:10.5194/acp-17-8371-2017.

Tohjima, Y., S. Maksyutov, T. Machida, and G. Inoue (1996), Airborne measurements of atmospheric methane over oil fields in western Siberia, *Geophys. Res. Lett.,* 23, 1621-1624.

Tohjima, Y., H. Wakita, S. Maksyutov, T. Machida, G. Inoue, N. Vinnichenko, and V. Khattatov (1997), Distribution of tropospheric methane over Siberia in July 1993, *J. Geophys. Res.,* 102, 25371-25382.

Tsuruta, A., T. Aalto, L. Backman, J. Hakkarainen, I. T. van der Laan-Luijkx, M. C. Krol, R. Spahni, S. Houweling, M. Laine, E. Dlugokencky, A. J. Gomez-Pelaez, M. van der Schoot, R. Langenfelds, R. Ellul, J. Arduini, F. Apadula, C. Gerbig, D. G. Feist, R. Kivi, Y. Yoshida, and

W. Peters (2017), Global methane emission estimates for 2000-2012 from CarbonTracker Europe-CH4 v1.0, *Geosci. Model Dev.,* 10, doi:10.5194/gmd-10-1261-2017.

Umezawa, T., T. Machida, S. Aoki, and T. Nakazawa (2012), Contributions of natural and anthropogenic sources to atmospheric methane variations over western Siberia estimated from its carbon and hydrogen isotopes, *Global Biogeochem. Cycles,* 26, doi:10.1029/2011GB004232.

Umezawa, T., D. Goto, S. Aoki, K. Ishijima, P. K. Patra, S. Sugawara, S. Morimoto, and T. Nakazawa (2014), Variations of tropospheric methane over Japan during 1988–2010, *Tellus B,* 66, doi:10.3402/tellusb.v66.23837.

Winderlich, J., H. Chen, C. Gerbig, T. Seifert, O. Kolle, J. V. Lavric, C. Kaiser, A. Hoefer, and M. Heimann (2010), Continuous low-maintenance CO_2/CH_4/H_2O measurements at the Zotino Tall Tower Observatory (ZOTTO) in Central Siberia, *Atmos. Meas. Tech.,* 3, doi:10.5194/amt-3-1113-2010.

Worthy, D. E. J., E. Chan, M. Ishizawa, D. Chan, C. Poss, E. J. Dlugokencky, S. Maksyutov, and I. Levin (2009), Decreasing anthropogenic methane emissions in Europe and Siberia inferred from continuous carbon dioxide and methane observations at Alert, Canada, *J. Geophys. Res.,* 114, doi:10.1029/2008JD011239.

Yamada, K., N. Yoshida, F. Nakagawa, and G. Inoue (2005), Source evaluation of atmospheric methane over western Siberia using double stable isotopic signatures, *Org. Geochem.,* 36, 717-726.

Figure 1. Map showing the 18 source regions in the tagged tracer experiments. Triangles in white and black indicate the location of Surgut and Novosibirsk, respectively. Colors show annual CH_4 emissions for 2009.

Figure 2. Temporal variation in CH_4 concentrations (black dots) observed over Surgut and their long-term trend lines. Green, blue, and red lines were calculated with the cutoff frequencies of 667, 1095, 1460 days, respectively (Section 2.4). Dotted curves indicate the range of estimated errors by the bootstrap method. Blue crosses denote STE-influenced samples that we did not use for the trend calculation.

Figure 3. Temporal variations in the growth rate (ppb yr^{-1}) of CH_4 concentrations for each altitude (m ASL) over Surgut and Novosibirsk. These lines were derivatives of the long-term trend lines with the cutoff frequency of 1460 days in Figure 2. Gray shades indicate the range of estimated errors by the bootstrap method (Section 2.4). Step lines and error bars indicate annual increases in globally-averaged CH_4 and its one SD, obtained from the network by NOAA (https://www.esrl.noaa.gov/gmd/ccgg/trends_ch4/).

Figure 4. Box and whisker plot of monthly variations in CH_4 concentrations relative to the long-term trend line calculated with the cutoff frequency of 1460 days over Surgut. The whiskers extend to the most extreme data point which is no more than 1.5 times the interquartile range from the box. Individual outliers are shown as crosses outside the whiskers.

Figure 5. Stacked chart for temporal variation of the contributions from 18 regions at four altitudes over Surgut.

Figure 6. Long-term trend in the contribution of 18 regions at 5.0 km and 1.0 km over Surgut. All data have applied the offset at the first data of 2001. The lines were calculated by the curve fitting method (Section 2.4). Gray shades indicate the range of estimated errors by the bootstrap method (Section 2.4).

Figure 7. (a) Temporal variation in the monthly means of contribution from Europe (red) and the WSL (blue) of the tagged simulation to the concentration at 1 km (solid line) and 5.5 km (dotted line) over Surgut. The monthly means were produced from the fitting method (Section 2.4) and offset by the first value of 5.5 km from each region. (b) Temporal variation in the vertical difference between 1 km and 5.5 km of the monthly mean values produced from the fitting method over Surgut. Horizontal dashed lines indicate the mean values during 1995-1999, 2002-2006, and 2009-2013. Area chart shows the vertical gradient calculated for emissions from Europe (pink), the WSL (light blue), and Boreal North America (gray). Horizontal red and blue lines indicate the mean values for Europe and the WSL, respectively, during 2002-2006 and 2009-2013.

Figure 8. (a) Temporal variation in the monthly means of contribution from Europe (red) and the WSL (blue) of the tagged simulation to the concentration at 1 km (solid line) and 5.5 km (dotted line) over Novosibirsk. The monthly means were produced from the fitting method (Section 2.4) and offset by the first value of 5.5 km from each region. (b) Temporal variation in the vertical difference between 1 km and 5.5 km of the monthly mean values produced from the fitting method over Novosibirsk. Horizontal dashed lines indicate the mean values during 2002-2006 and 2009-2013. Area chart shows the vertical gradient calculated for emissions from Europe (pink), the WSL (light blue), and Boreal North America (gray). Horizontal red and blue lines indicate the mean values for Europe and the WSL, respectively, during 2002-2006 and 2009-2013.

Figure 9. (a) Mean vertical profile of CH_4 concentrations over Surgut for the periods of 1995-1999, 2002-2006, and 2009-2013. The data were offset by the mean values of 5.5 km in each period. Error bars indicate standard errors. Closed and open symbols indicate observed and total simulated data, respectively. Contribution from (b) Europe, the (c) WSL, and (d) Boreal North America are shown for the periods of 2002-2006 and 2009-2013.

Table 1. Sampling information and experiment setup

Site name	Sampling date	Flask size (mL)	Instrument type
Surgut	July 23, 1993-Sep. 28, 2002	550	GC-9A
	Oct. 31, 2002- Feb. 22, 2005	550	Agilent 6890
	Mar. 23, 2005-Apr. 26, 2012	500, 750	HP5890
	May 24, 2012-Jan. 28 2014	750	HP5890
	Apr. 24 2014-	750	Agilent 7890A
Novosibirsk	July 23, 1997-May 28, 1999	500	HP5890
	June 30, 1999-Feb. 18, 2004	500, 750	HP5890
	Mar. 17, 2004-Jan. 30, 2014	750	HP5890
	Mar. 18, 2014-	750	Agilent 7890A

Scale	Precision (ppb)	Institution
TU scale	3	Tohoku University
TU scale	2	Tohoku University
NIES 94 CH4 scale	1.7	NIES
NIES 94 CH4 scale	1.7	NIES
NIES 94 CH4 scale	1.7	NIES
NIES 94 CH4 scale	1.7	NIES
NIES 94 CH4 scale	1.7	NIES
NIES 94 CH4 scale	1.7	NIES
NIES 94 CH4 scale	1.7	NIES

Figure 1.

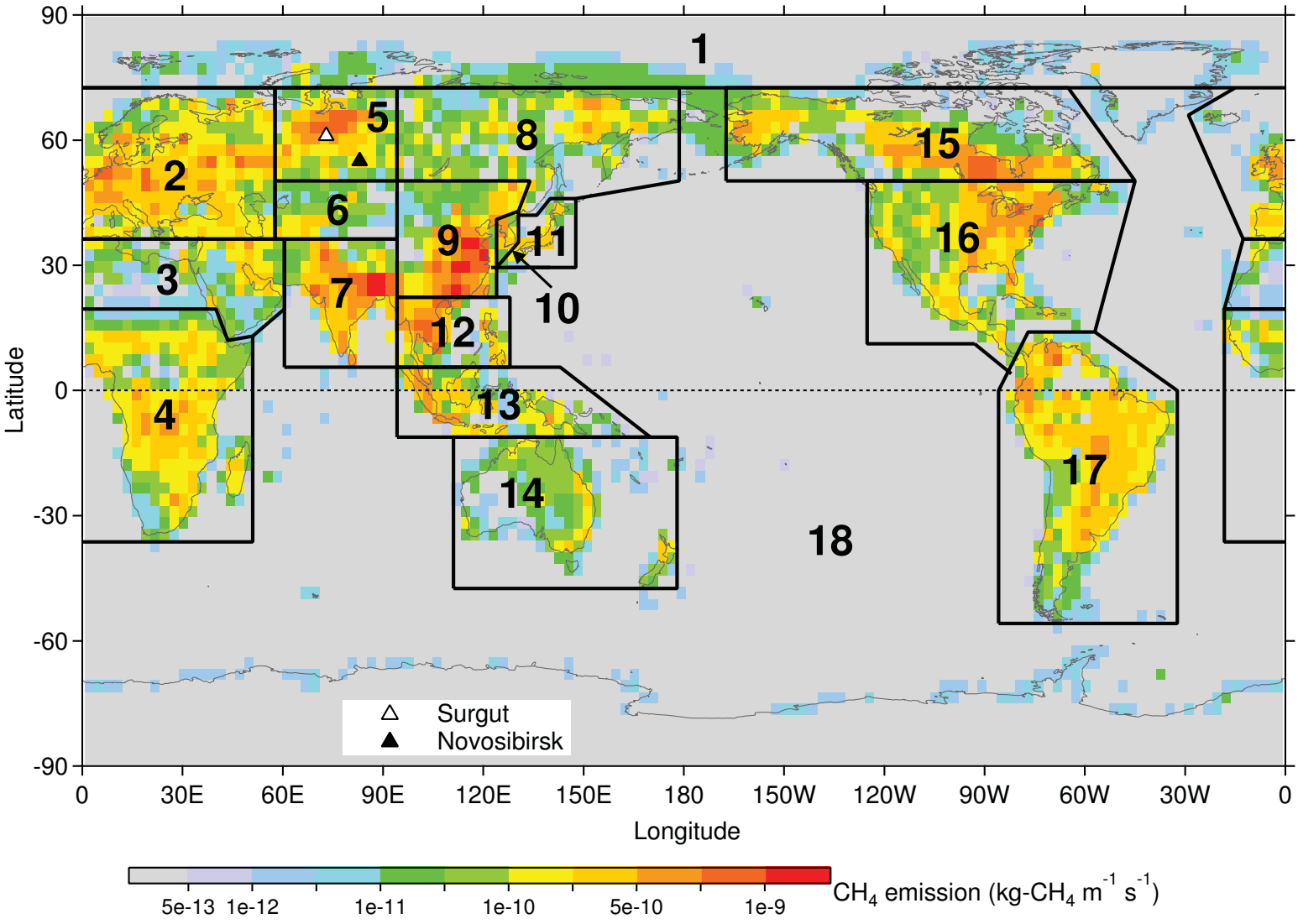
90
60
30
0
-30
-60
-90
Latitude
0
30E
60E
90E
120E
150E
180
150W
120W
90W
60W
30W
0
Longitude
1
2
3
4
5
6
7
8
9
10
11
12
13
14
15
16
17
18
Surgut
Novosibirsk
5e-13
1e-12
1e-11
1e-10
5e-10
1e-9
CH4 emission (kg-CH4 m-1 s-1)

Figure 2.

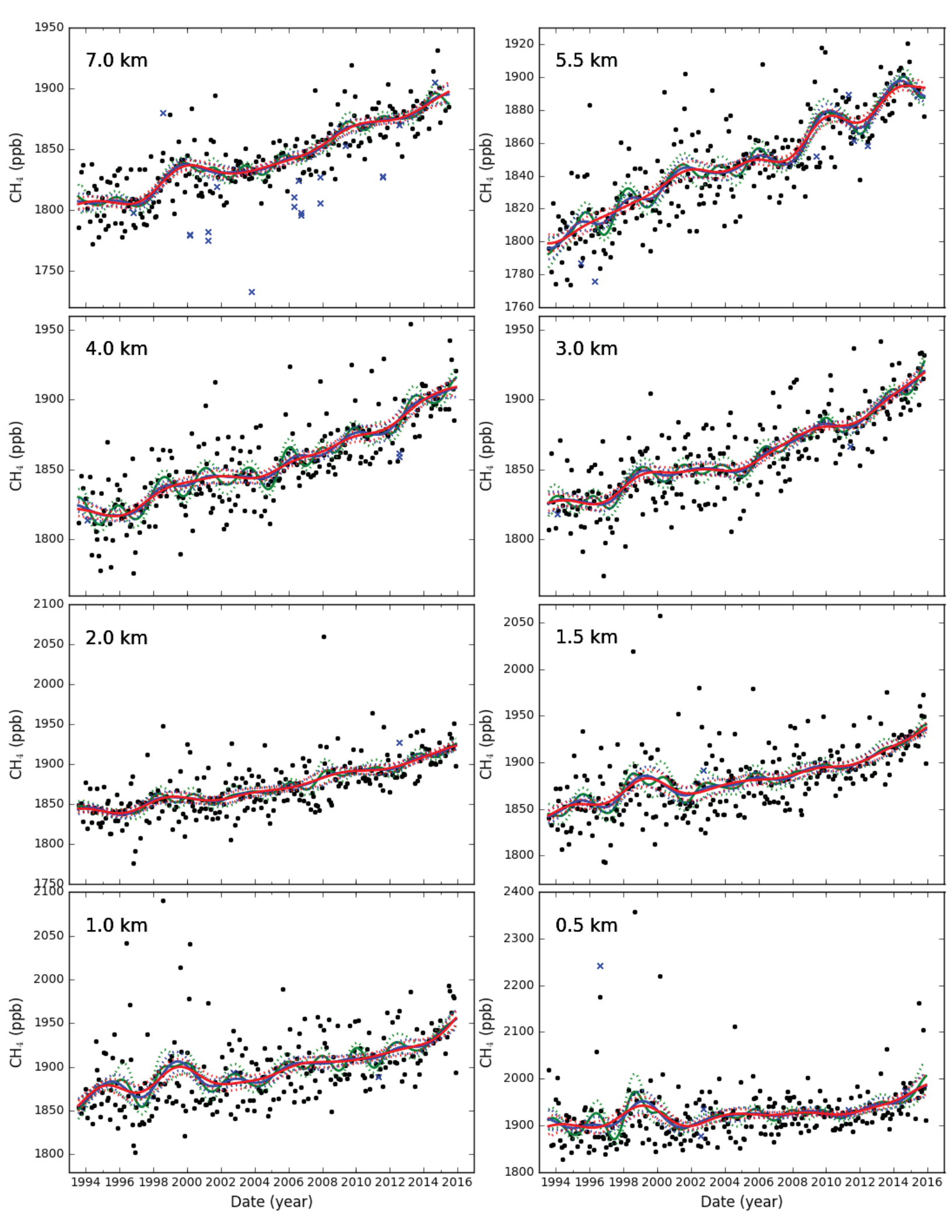
7.0 km
5.5 km
4.0 km
3.0 km
2.0 km
1.5 km
1.0 km
0.5 km
CH4 (ppb)
Date (year)
1994 1996 1998 2000 2002 2004 2006 2008 2010 2012 2014 2016

Figure 3.

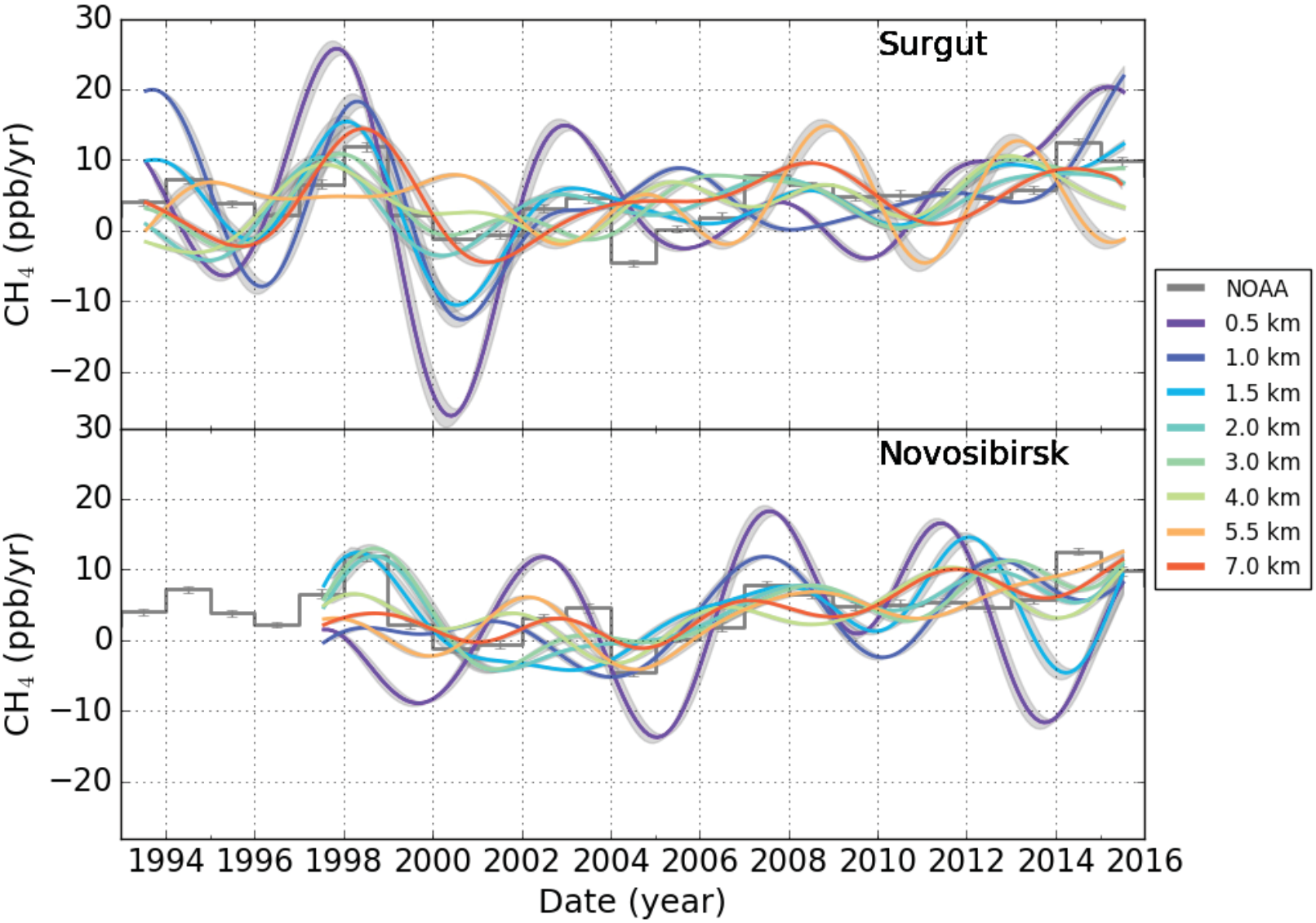
Surgut
Novosibirsk
CH_4 (ppb/yr)
30
20
10
0
−10
−20
1994 1996 1998 2000 2002 2004 2006 2008 2010 2012 2014 2016
Date (year)
NOAA
0.5 km
1.0 km
1.5 km
2.0 km
3.0 km
4.0 km
5.5 km
7.0 km

Figure 4.

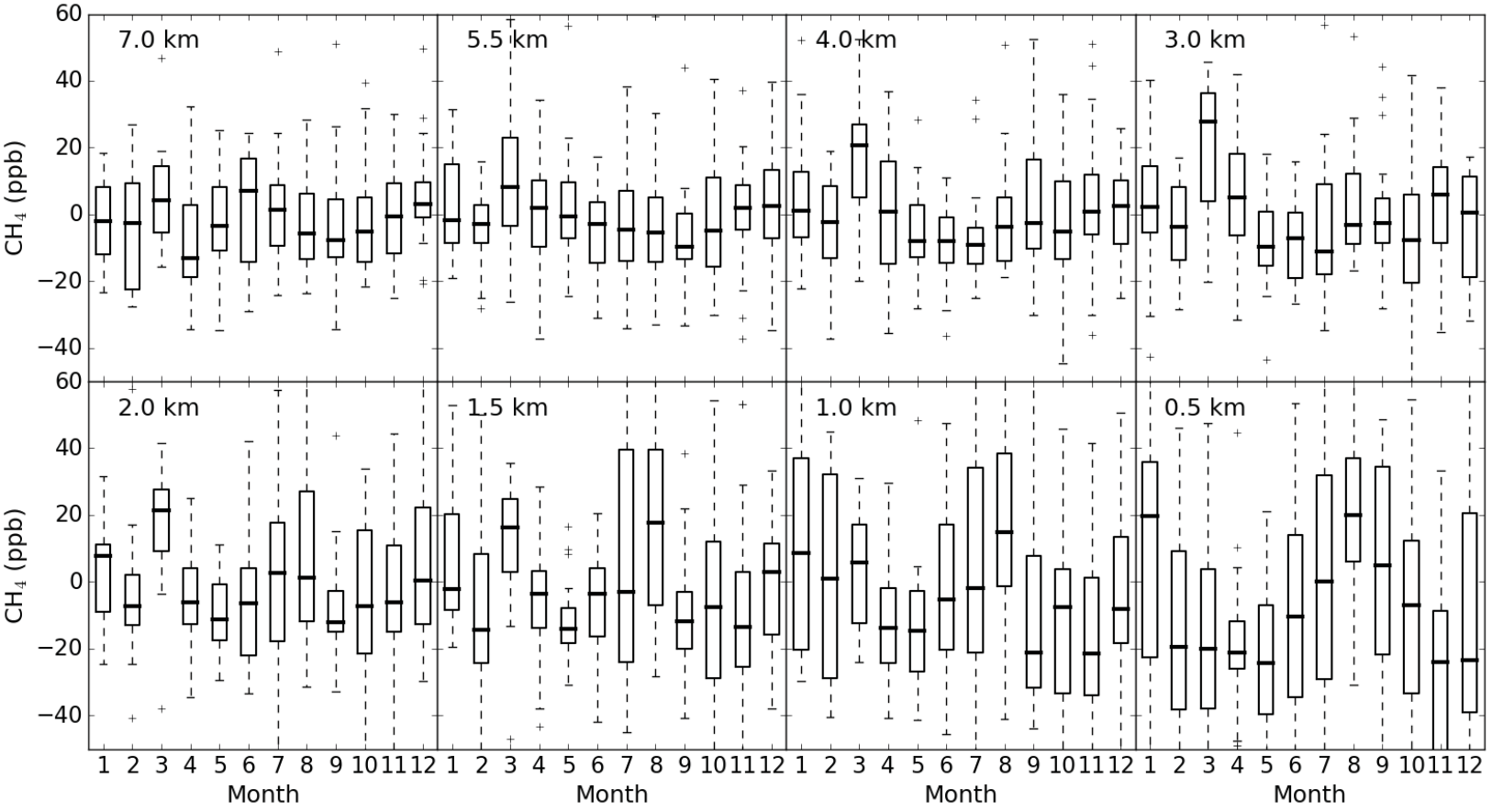
7.0 km
5.5 km
4.0 km
3.0 km
2.0 km
1.5 km
1.0 km
0.5 km
CH4 (ppb)
CH4 (ppb)
60
40
20
0
−20
−40
1 2 3 4 5 6 7 8 9 10 11 12
Month

Figure 5.

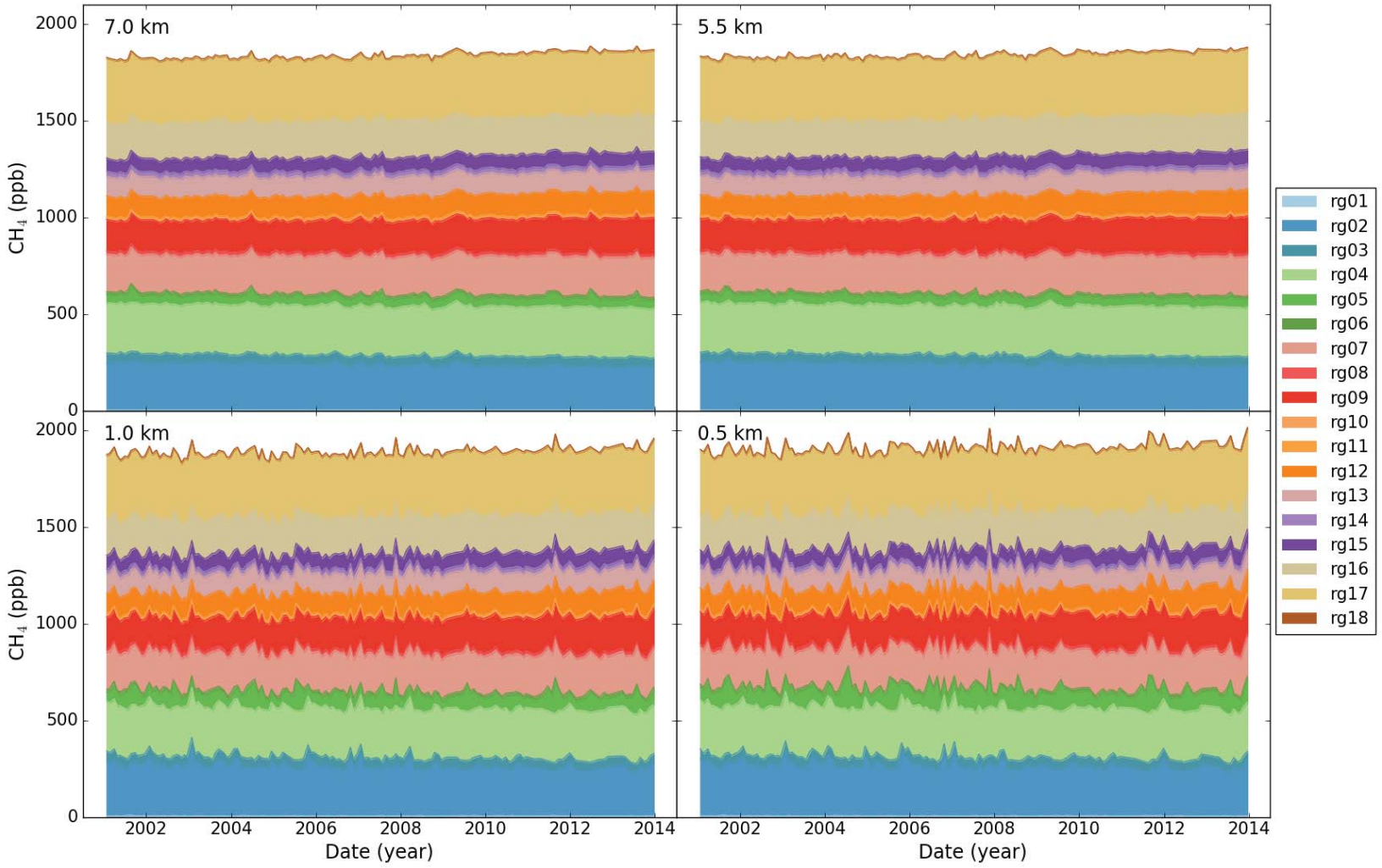
7.0 km
5.5 km
1.0 km
0.5 km
CH4 (ppb)
0
500
1000
1500
2000
2002
2004
2006
2008
2010
2012
2014
Date (year)
rg01
rg02
rg03
rg04
rg05
rg06
rg07
rg08
rg09
rg10
rg11
rg12
rg13
rg14
rg15
rg16
rg17
rg18

Figure 6.

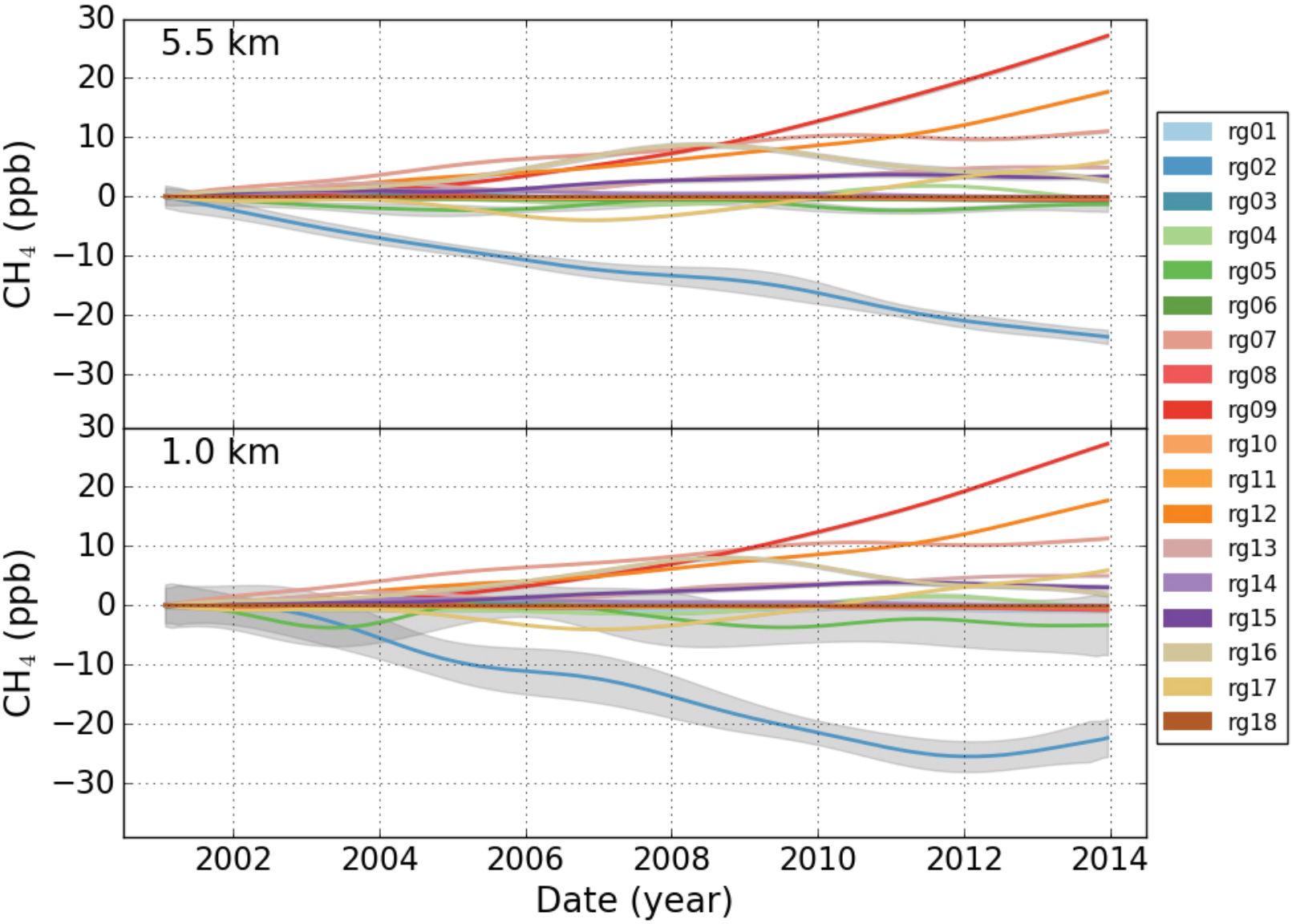
5.5 km
1.0 km
CH4 (ppb)
CH4 (ppb)
30
20
10
0
−10
−20
−30
2002
2004
2006
2008
2010
2012
2014
Date (year)
rg01
rg02
rg03
rg04
rg05
rg06
rg07
rg08
rg09
rg10
rg11
rg12
rg13
rg14
rg15
rg16
rg17
rg18

Figure 7.

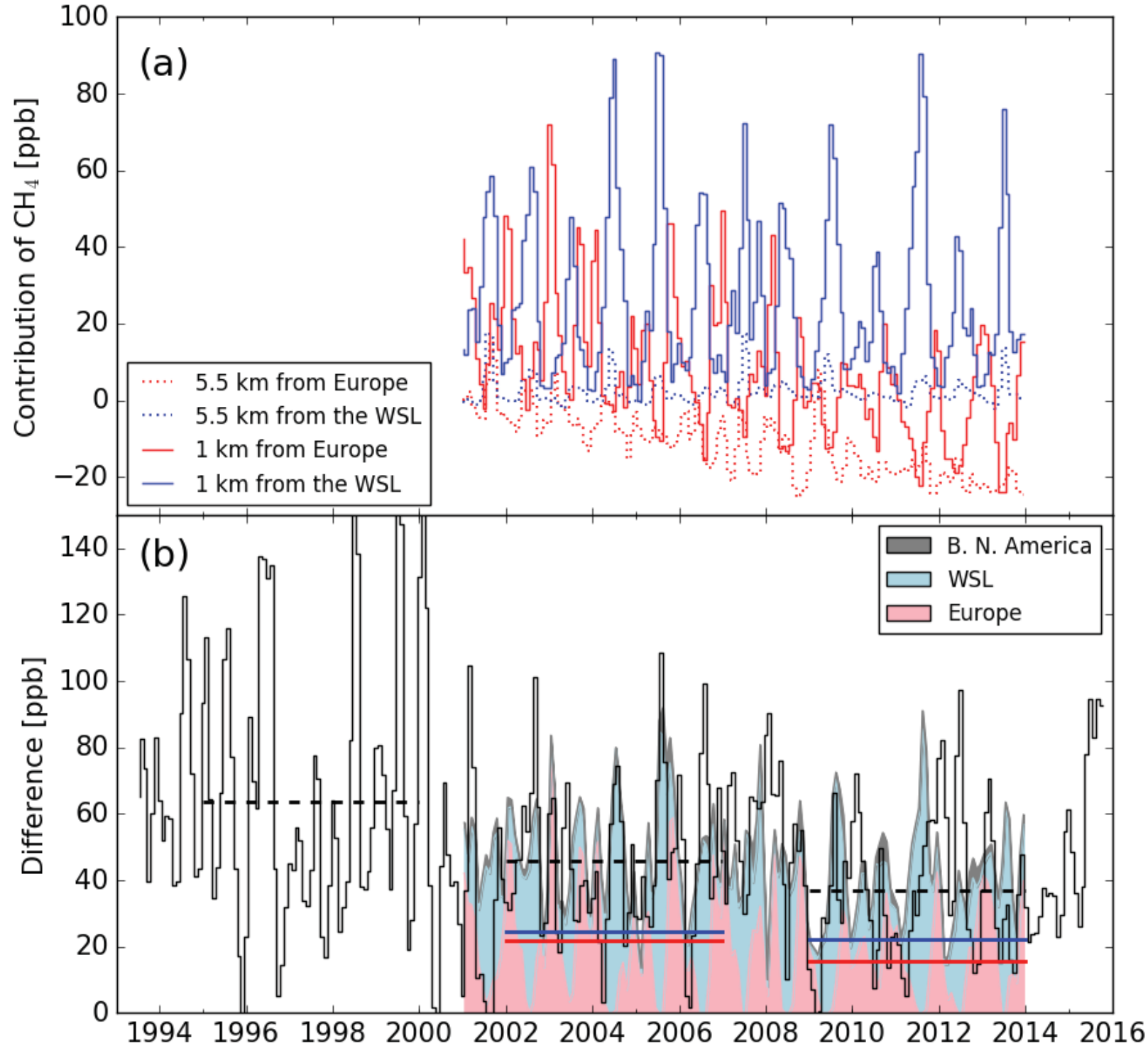
(a)
Contribution of CH_4 [ppb]
100
80
60
40
20
0
−20
5.5 km from Europe
5.5 km from the WSL
1 km from Europe
1 km from the WSL
(b)
Difference [ppb]
140
120
100
80
60
40
20
0
B. N. America
WSL
Europe
1994
1996
1998
2000
2002
2004
2006
2008
2010
2012
2014
2016

Figure 8.

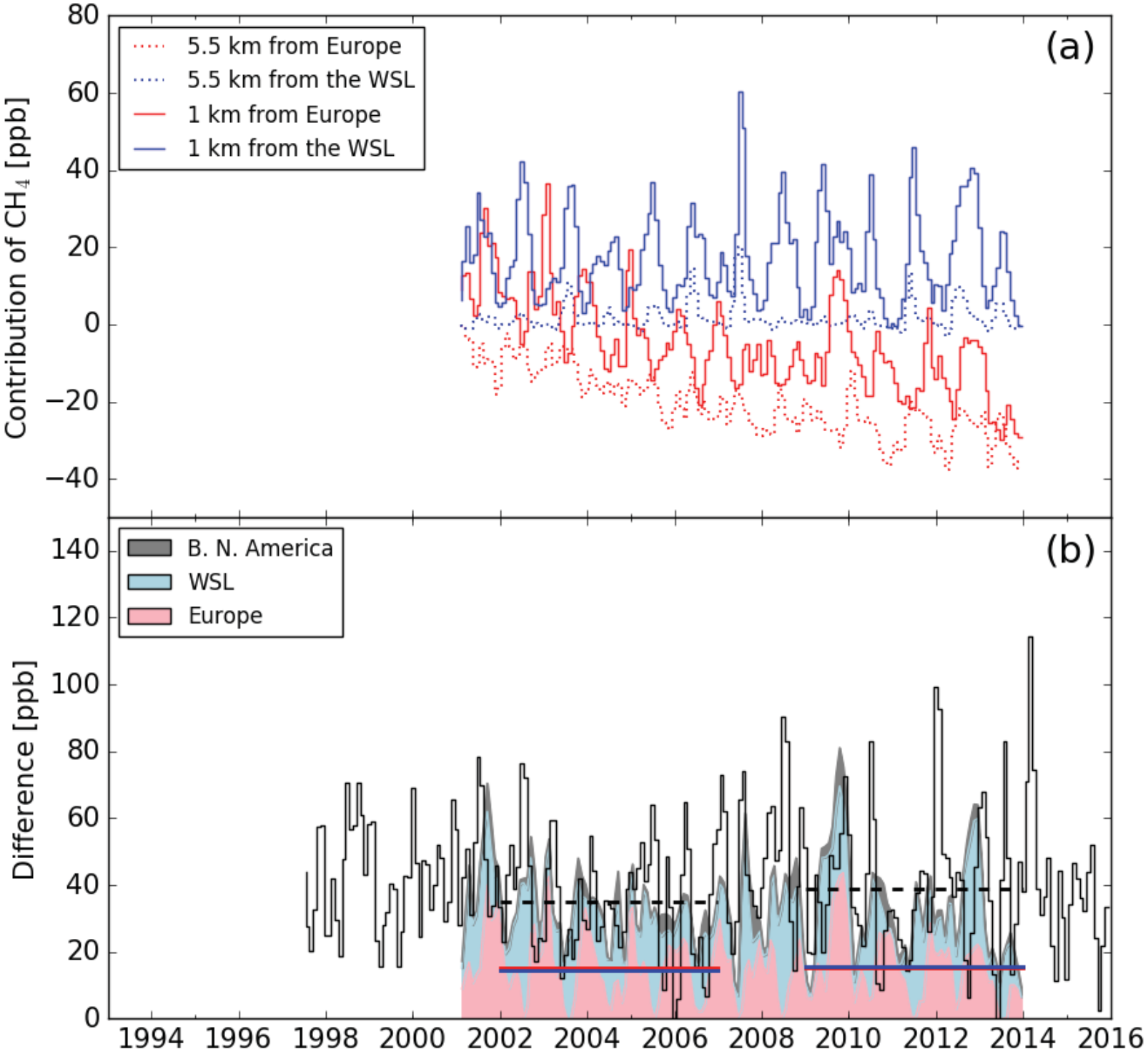
(a)
5.5 km from Europe
5.5 km from the WSL
1 km from Europe
1 km from the WSL
Contribution of CH_4 [ppb]
80
60
40
20
0
−20
−40
(b)
B. N. America
WSL
Europe
Difference [ppb]
140
120
100
80
60
40
20
0
1994
1996
1998
2000
2002
2004
2006
2008
2010
2012
2014
2016

Figure 9.

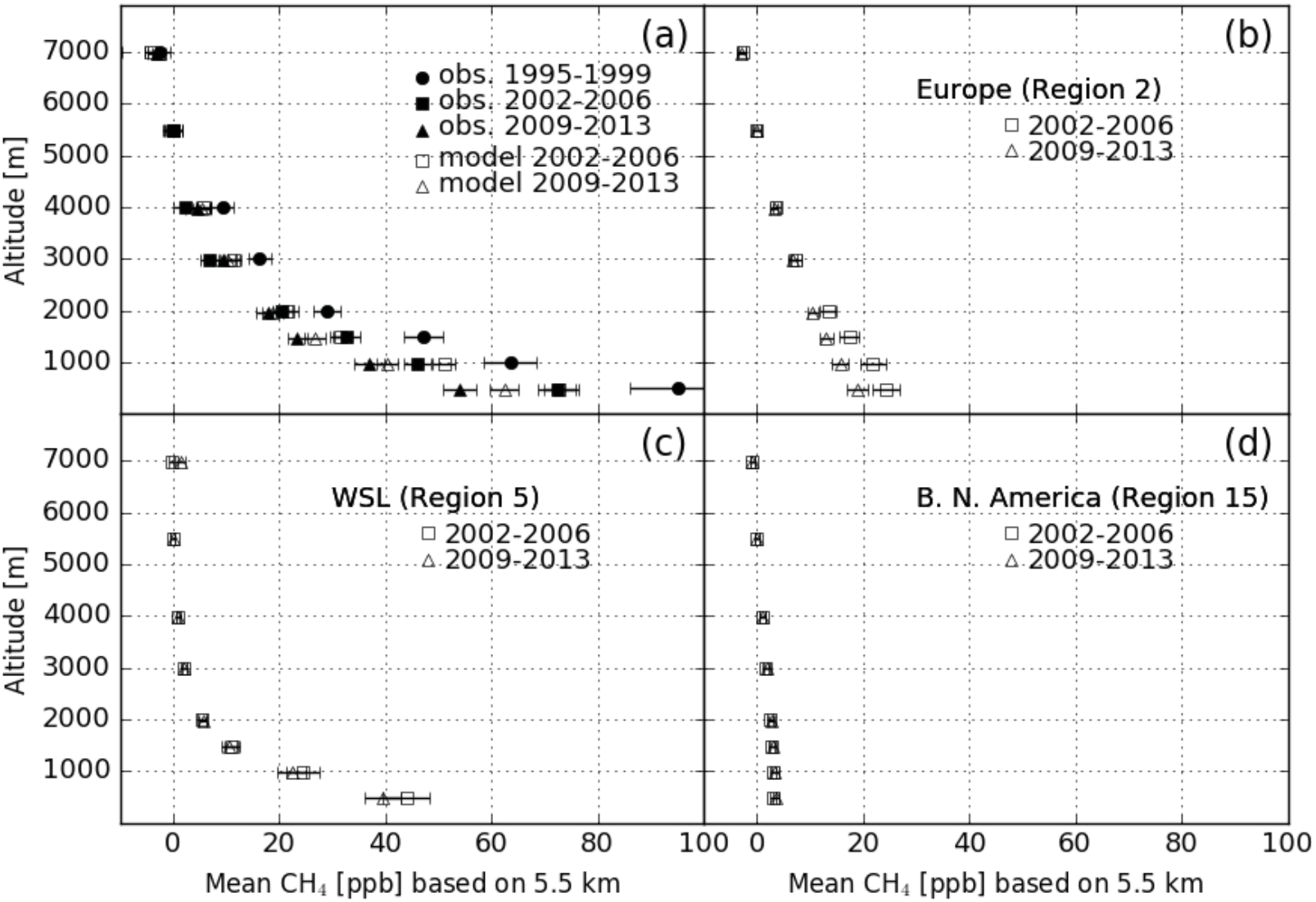
(a)
obs. 1995-1999
obs. 2002-2006
obs. 2009-2013
model 2002-2006
model 2009-2013
(b)
Europe (Region 2)
2002-2006
2009-2013
(c)
WSL (Region 5)
2002-2006
2009-2013
(d)
B. N. America (Region 15)
2002-2006
2009-2013
Altitude [m]
Mean CH4 [ppb] based on 5.5 km